Adsorption of anionic dyes from aqueous solution on zeolite from fly ash-iron oxide magnetic nanocomposite

D. A. Fungaro[*], M. Yamaura, and T. E. M. Carvalho

Chemical and Environmental Technology Center, Nuclear and Energy Research Institute, P.C. 11049, São Paulo, Brazil

Abstract. Magnetic zeolite/iron oxide nanocomposite was prepared by mixing zeolite synthesized from coal fly ashes with magnetite nanoparticles in suspension and was used for the removal of Reactive Orange 16 (RO16) and Indigo Carmine (IC) from aqueous solutions. The effect of various experimental parameters such as contact time, pH, adsorbent dose and temperature were investigated. The experimental data were analyzed using the pseudo-first-order and pseudo-second-order adsorption kinetic models. The experimental data fit the second-order kinetic model. The Langmuir and Freundlich isotherm models were tested for their applicability. Results indicated that according to the Langmuir isotherm, the maximum sorption capacities are 1.1 and 0.58 $mg \cdot g^{-1}$ for RO16 and IC, respectively. Thermodynamic parameters showed that adsorption of dyes were endothermic and spontaneous in nature.

1 Introduction

Magnetic separation technology as an efficient, fast and economical method for separating magnetic materials has been widely used in textile, biology, and environmental protection [1–4]. Adsorption is considered a simple and economical technique for wastewater treatment [5,6].

The adsorbents combining magnetic separation technology with adsorption process have been widely used in environmental purification [7–9]. The main advantage of this technology is that it can dispose a mass of wastewater in a very short period of time and produce no contaminants such as flocculants [10]. Some examples are the use of activated carbon/iron oxide

---

[*]Corresponding author. *Email address:* `dfungaro@ipen.br` (D. A. Fungaro)

magnetic composites for the adsorption of volatile organic compounds [11], montmorillonite-iron oxide magnetic composites for the adsorption of metal cations [12] and NaY zeolite- iron oxide magnetic composite for removal of metallic contaminants from aqueous solution [13].

Most commercially available magnetic particles are rather expensive and cannot be used for large-scale processes. Magnetic modification of low cost adsorbents could lead to materials suitable for biotechnology and environmental applications.

Zeolite synthesized from Brazilian coal fly ashes offer an attractive and inexpensive material option for removal of contaminants. In our group zeolites synthesized from Brazilian coal fly ashes have been used as low-cost adsorbents to remove contaminants from aqueous effluents [14,15] and zeolite from fly ash/iron oxide composites were used as adsorbents for the removal of metal ions of Zn^{2+}, Cd^{2+} and Pb^{2+} from water [16,17].

In the present study, magnetic nanocomposite of zeolite from fly ash was prepared by simple method and their adsorptive characteristic for the removal of dyes from aqueous solution was studied. The adsorption studies such as effect of contact time, pH, adsorbent dose and temperature were explored in batch experiments and thermodynamic, kinetic and adsorption isotherm analysis were used to elucidate the adsorption mechanism.

2 Materials and methods

2.1 Materials

All chemicals used in this study were of analytical grade. Reactive Orange 16 (RO16; C.I. 17757; $C_{20}H_{17}N_3O_{10}S_3Na_2$; molar mass = 601.54 g·mol^{-1}) was purchased from Sigma-Aldrich (50% purity) and Indigo Carmine (IC; C.I. 73015; $C_{16}H_8N_2Na_2O_8S_2$; molar mass = 466.35 g·mol^{-1}) was supplied by Vetec Quimica Fina Ltda (100% purity). Stock solutions were prepared in deionized water (Millipore Milli-Q) and the solutions for adsorption tests were prepared by diluting. The sample of coal fly ashes from baghouse filter was obtained from a coal-fired power plant located at Figueira City, in Parana State, Brazil.

2.2 Preparation of the zeolite from fly ash-iron oxide magnetic composite

First, coal fly ash was used as starting material for zeolite synthesis by means of hydrothermal treatment. In synthesis experiment, 20 g of fly ash was heated to 100 °C in an oven for 24 h with 160 mL of 3.5 mol·L^{-1} NaOH solution. The zeolitic material (ZC) was repeatedly washed with deionized water until pH 11 and dried at 100 °C for 24 h [18]. Magnetite particles were prepared by adding of NaOH solution drop by drop into ferrous sulfate solution with agitation until the pH reached 11. The slurry was heated on a water bath. After that, the magnetite was washed with distilled water and dried at room temperature. The magnetite particles were redispersed in aqueous solution and ZC was added slowly with agitation. The zeolite ZC/magnetite ratio was 3:1(w/w). The obtained zeolite-iron oxide magnetic composite (ZM) was washed with distilled water, dried at room temperature and milled. The black product was attracted toward the magnet (Fig. 1).
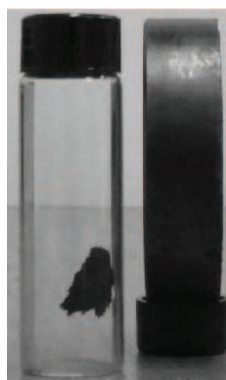
Figure 1: Photograph of the attraction process of zeolite-iron oxide composite by a magnet.

2.3   Adsorption studies

The adsorption was performed using the batch procedure. Kinetic experiments were carried out by shaking 50 mg of adsorbent with 5 mL of dye solutions with initial concentration of 10.0 mg·L^{-1} at room temperature (25 $\pm$ 2 °C) in a shaker operated at 360 rpm for 30–420 min in glass bottles. Samples were withdrawn at appropriate time intervals and placed on top of a magnet for 60 min to settle the particles and 4 ml of supernatant was taken for the measurement. The concentration of dye in the supernatant solution was analyzed using a UV spectrophotometer (Cary 1E – Varian) by measuring wavelength of maximum absorption at 493 nm for RO16 and 610 nm for IC. The same experiment was repeated with variations in some of the parameters such as: pH (2–10), mass of adsorbent (25–150 mg) and temperature (293, 303 and 313 K). Each experiment was duplicated under identical conditions. The adsorption capacity (mg·g^{-1}) of adsorbents was calculated from

$$q_e = \frac{(C_0 - C_e)V}{M}, \tag{1}$$

where q_e is the adsorbed amount of dye per gram of adsorbent, C_0 and C_e the concentrations of the dye in the initial solution and equilibrium, respectively (mg·L^{-1}); V the volume of the dye solution added (L) and M the amount of the adsorbent used (g).

For adsorption isotherms, samples with concentrations ranging from 1.2 to 20.0 mg·L^{-1} for RO16 and 2.7 to 19.5 mg·L^{-1} for IC were agitated till the equilibrium was achieved. The equilibrium data obtained in the present study were analyzed using the linear forms of the expressions of Langmuir (Eq. (2)) and Freundlich (Eq. (3)) isotherm models

$$\frac{C_e}{q_e} = \frac{1}{Q_0 b} + \frac{C_e}{Q_0}, \tag{2}$$

$$\log q_e = \log K_F + \frac{1}{n} \log C_e, \tag{3}$$

where C_e is the equilibrium concentration (mg·L^{-1}), q_e the amount adsorbed at equilibrium (mg·g^{-1}), Q_0 is the maximum amount of adsorbate per unit weight of adsorbent to form a complete monolayer on the surface (mg·g^{-1}); b is the Langmuir isotherm constant (L·mg^{-1}), related to the affinity of the adsorption sites; KF [(mg·g^{-1}) (L·mg^{-1})$^{1/n}$ and n are the Freundlich constants related to adsorption capacity and adsorption intensity of adsorbents, respectively.

The non-linear regression Chi-square (χ^2) test was employed as a criterion for the fitting quality due to the inherent bias resulting from linearization of isotherm models. This statistical analysis is based on the sum of the squares of the differences between the experimental and model calculated data, of which each squared difference was divided by the corresponding data obtained by calculating from models [19]. The Chi-square can be represented by

$$\chi^2 = \sum \frac{(q_e\exp - q_e\text{calc})^2}{q_e\text{calc}}, \tag{4}$$

where $q_e\exp$ is the equilibrium capacity of the adsorbent obtained from experiment (mg·g^{-1}), and $q_e$calc is the equilibrium capacity obtained by calculating from the model (mg·g^{-1}). A low value of χ^2 indicates that experimental data fit better to the value from the model. Therefore, it is necessary to analyze the data set using the Chi-square test to confirm the best fit isotherm for the adsorption system combined with the values of the correlation coefficient.

3   Results and discussion

3.1   Kinetic studies

Fig. 2 shows the effect of contact time on the adsorption capacities of RO16 and IC by ZM. It is clear that the adsorption capacity of ZM increased rapidly in the initial stages of contact time and gradually increased with prolonging the contact time until equilibrium. It can be seen that the adsorption equilibrium of RO16 and IC on ZM were reached at 300 and 360 min, respectively.

In order to investigate the adsorption processes of RO16 and IC by ZM pseudofirst- order (Eq. (5)) and pseudo-second-order kinetic (Eq. (6)) models were used with equations as follows

$$\log(q_e - q_t) = \log - \frac{k_1 t}{2.303}, \tag{5}$$

$$\frac{t}{q_t} = \frac{1}{k_2 q_e^2} + \frac{1}{q_e} t, \tag{6}$$

where q_e is the amount of dye adsorbed at equilibrium (mg·g^{-1}), q_t is the amount of dye adsorbed at time t (mg·g^{-1}), k_1 is the rate constant of the pseudo-first-order sorption (min^{-1}), and k_2 is the rate constant of the pseudo-second-order kinetics (g·mg^{-1} ·min^{-1}) [20,21].
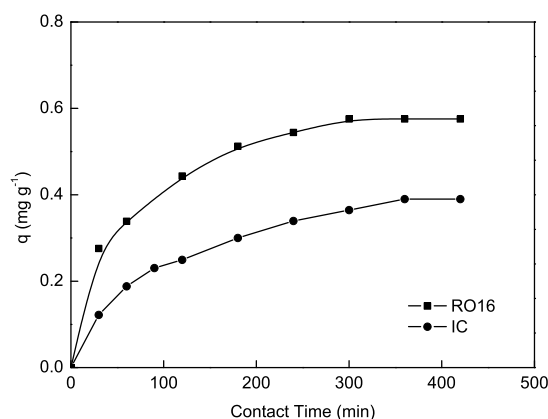
Figure 2: Effect of contact time on the adsorption of RO16 and IC by ZM.

The possibility of intraparticle diffusion resistance affecting adsorption was explored using the appropriate intraparticle diffusion model as [22]

$$q_t = k_{id} t^{\frac{1}{2}} + C, \tag{7}$$

where k_{id} is the intraparticle diffusion rate constant (mg·g^{-1}·min$^{1/2}$). According to Eq. (7), a plot of q_t versus $t^{1/2}$ should be a straight line with a slope k_{id} and intercept C when adsorption mechanism follows the intraparticular diffusion process. Values of the C give an idea about the thickness of boundary layer, i.e., the larger the intercept is the greater the boundary layer effect.

The calculated kinetic constants values and the corresponding linear regression correlation constants are given in Table 1. The pseudo second-order kinetic model better describes all of the dyes adsorption according to the correlation coefficients ($R_2 \geq 0.99$) than those of pseudo first-order model. In addition, the experimental adsorption capacity values were very close to the model-calculated adsorption capacity data (not shown), verifying the high correlation of adsorption to the pseudo-second-order model. The fitted linear regression plots of pseudo-second-order model are shown in Fig. 3.

The plots of intraparticle diffusion of RO16 and IC onto the ZM are illustrated in Fig. 4. The linearity of fitting lines in plots points to the presence of intraparticle diffusion. However, the deviation of the lines from the origin indicates that the pore diffusion is not the only rate controlling step [22, 23]. As the plot is often multi linear for many adsorption systems, it is common to segment it into two or more straight lines and to assume that different adsorption mechanisms control the step represented by each straight line [24]. Referring to RO16/ZM system, two distinct regions are observed (Fig. 4a). The first section of plots indicates that boundary layer diffusion probably limited dye adsorption. The second section shows the occurrence of intraparticle diffusion as the adsorption limiting step [25, 26].

Table 1: Kinetic parameters for the adsorption of dyes onto ZM.

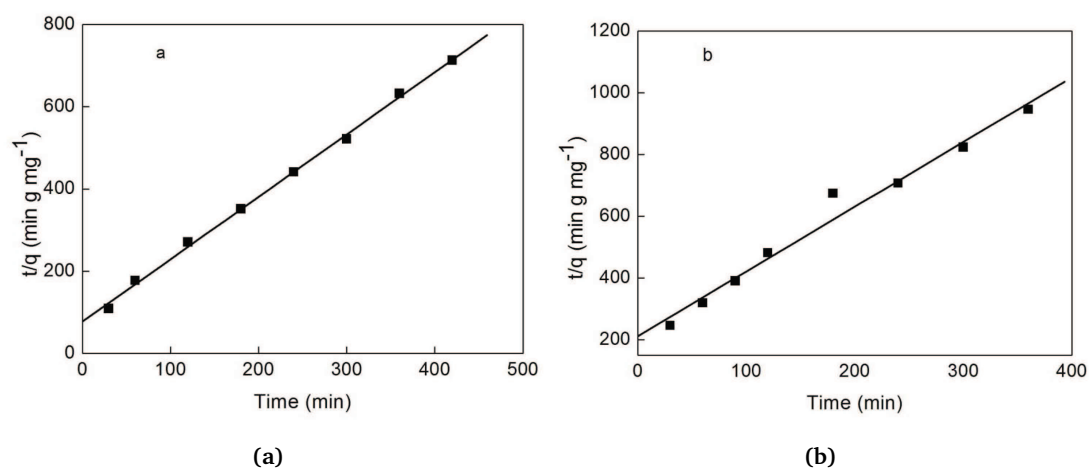| Dyes	Pseudo first-order			
	k_1 ($\min^{-1}$)	R_1		
RO16	1.15×10^{-2}	0.9954		
IC	0.94×10^{-2}	0.9734		
	Pseudo second-order			
	k_2 (g·mg^{-1}·min^{-1})	h (mg·g^{-1}·min^{-1})	q_e (mg·g^{-1})	R_2
RO16	3.90×10^{-2}	1.29×10^{-2}	0.659	0.9991
IC	2.08×10^{-2}	0.47×10^{-2}	0.477	0.9894
	Intraparticle diffusion			
	C (mg·g^{-1})	k_i (mg·g^{-1}·min$^{\frac{1}{2}}$)	R_i	
RO16	0.251	2.83×10^{-3}	0.9556	
IC	0.037	1.87×10^{-2}	0.9975	

Figure 3: Pseudo-second order adsorption kinetics of (a) RO16, (b) IC on ZM.

The absence of such features in the plot of IC/ZM system (Fig. 4b) indicated that the steps were indistinguishable from one another and that the intraparticle diffusion was a prominent process [27].

3.2 Adsorption isotherms

The isotherm parameters for RO16 and IC of two models are presented in Table 2. The isotherms of the two dyes with the experimental data points and the two theoretical isotherms plotted on the same graph are given in Fig. 4.
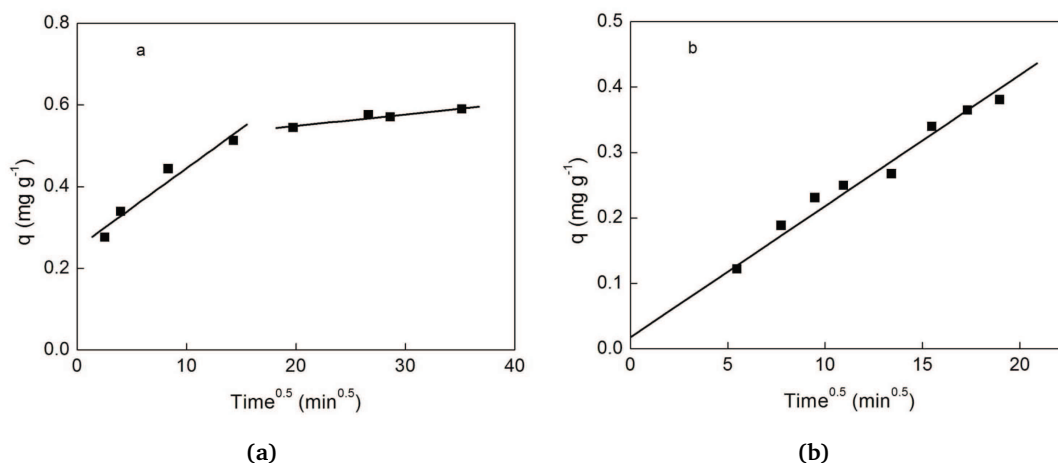
Figure 4: Intraparticle diffusion model of (a) RO16, (b) IC on ZM.

Table 2: Langmuir and Freundlich parameters for the adsorption of RO16 and IC onto ZM.

| Dye | Langmuir | | | |
	Q_0 (mg·g^{-1})	b (L·mg^{-1})	R	χ^2
RO16	1.06	0.582	0.9843	0.1691
IC	0.583	0.359	0.9880	0.03817
	Freundlich			
	K_f [(mg·g^{-1})(L·mg^{-1})$^{1/n}$]	n	R	χ^2
RO16	0.34	2.00	0.8736	0.4523
IC	0.191	2.68	0.9722	0.01608

The Langmuir isotherm gave a better fit than the Freundlich isotherm by giving greater R value closer to unity (0.98) and smaller value of χ^2 for RO16 adsorption by ZM. For IC, the correlation coefficients for the Freundlich model and the Langmuir model are much similar but according to the χ^2 values, the best-fit isotherm model was the Freundlich isotherm model [19]. The value of n, which is significantly higher than unity, indicated that both RO16 and IC dyes are favourably adsorbed by zeolitic material for under the experimental condition [28].

In general for the adsorption process, the degree of adsorption depends on both the active sites of the adsorbent and the adsorbate properties. An interaction occurs between active sites on zeolite-iron oxide magnetic nanocomposite (Si–O and O–H) and SO_3^-, –N=N– and –N=C–C=C– groups and aromatic skeletal vibrations of dyes [25, 29, 30].

3.3 Effect of solution pH

The pH was shown to be an important parameter in terms of the adsorption capacity, influencing not only the surface charge of the adsorbent but also the level of ionization of the material

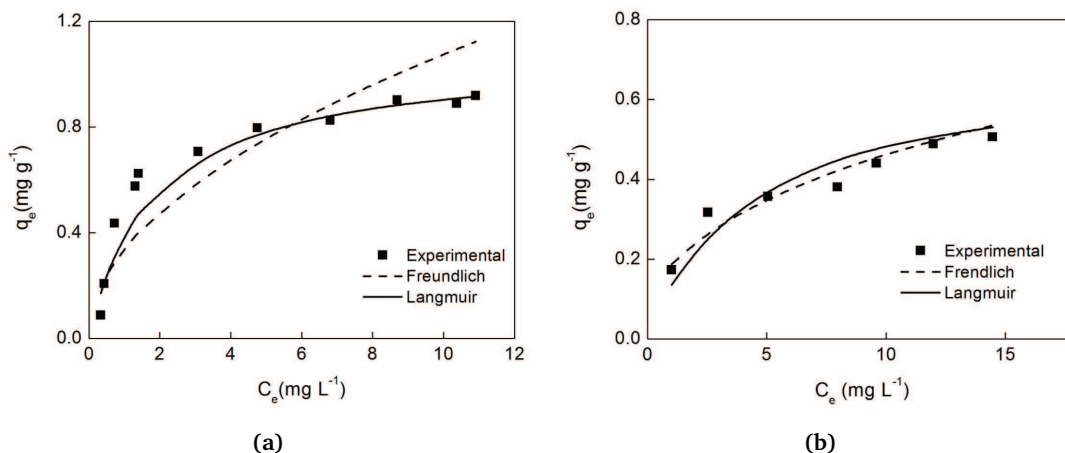**(a)**   **(b)**

Figure 5: Adsorption isotherms of dyes onto ZM: (a) RO16; (b) IC.

present in the solution. The effect of initial pH values for the adsorption of RO16 and IC dyes in solution onto ZM was investigated in the range of pH 2.0–10.0 (Fig. 6).

The adsorption of RO16 dyes on ZM is controlled by a pH-independent adsorption mechanism. The fact that the adsorption of dye onto zeolite from fly ash composite is not significantly affected with changing of initial pH of the dye solution may be attributed to the weak electrostatic interaction between the dye molecules and the sites on the surface of the zeolite particles [31] and neither the chemical species present in solution nor the effects of pH on the material superficies are important parameters for the adsorption processes.

It can be seen that the adsorption of IC was pH-dependent (Fig. 6). The amount adsorbed decreased as pH decreased from 2 to 4 and from 10 to 8 and remained constant in the pH
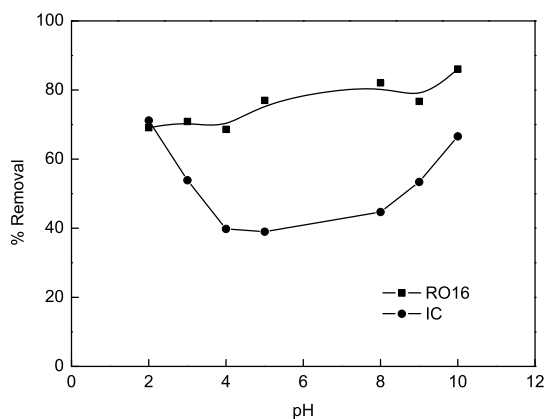

Figure 6: Effect of initial solution pH on dyes removal.

interval between 4 to 8. The chemical species has an important effect on the adsorption of indigo carmine on the magnetic composite. Indigo carmine may undergo a redox process involving the uptake of one proton per electron transferred or two protons per two electrons transferred. Transfer of the second electron results in formation of the hydroquinone [32]. These results may indicate that the species present interacts with the adsorbent and the interactions between IC and composite surface can occurs due electrostatic force and weak interaction of van der Walls forces. Previous studies have demonstrated that another possible interaction mechanism of the IC with magnetic zeolitic material composite is catalytic degradation [32,33].

3.4 Adsorbent dosage

The study of adsorbent mass for the removal of dyes from aqueous solution was carried out using adsorbent masses ranging from 25 to 150 mg of ZM and fixing the initial dye concentration (Fig. 7). The highest amount of dye removal was attained for adsorbent masses of at least 50 mg for RO16 (Fig. 7a). For adsorbent dosages higher than this value, the percentage of dye removal remained almost constant. The increases in the adsorption with the dose can be attributed to increase surface area and the availability of more adsorption as already reported in several papers [34,35].

On the other hand, the increase in the adsorbent masses promoted a remarkable decrease in the amount of dye uptake per gram of adsorbent (q_e). The drop in adsorption capacity is basically due to sites remaining unsaturated during the adsorption and particle aggregation [36,37]. This effect can be also mathematically explained by combining of equations [38].

For IC, along with the increase of sorbent dosage from 25 to 150 mg, the percentage of dye removal increased and the adsorption equilibria was reached at 100 mg (Fig. 7b)
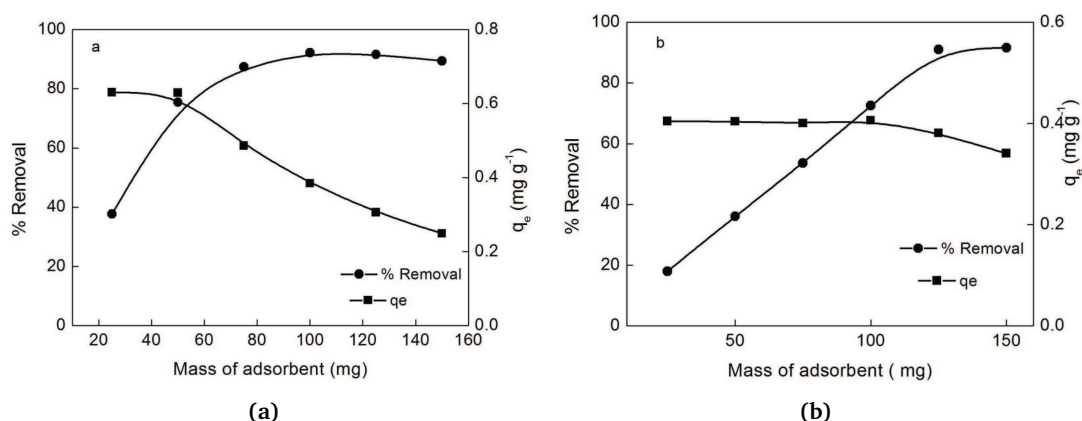

Figure 7: Effect of adsorbent mass on the percentage of removal and amount of dye adsorbed on ZM: (a) RO16; (b) IC.

3.5   Effect of temperature

As the temperature can influence the final value of adsorption, the study of its effects on the adsorption process becomes an important aspect in waste water treatment. The variation was explained on the basis of thermodynamic approach. The thermodynamic parameters, ΔG°, ΔH° and ΔS°, were calculated with the help of following equations

$$K_C = \frac{C_A}{C_S}, \tag{8}$$

$$\Delta G^\circ = -2{,}303 RT \log K_C, \tag{9}$$

$$\Delta H^\circ = 2{,}303 R \left(\frac{T_1 T_2}{T_2 - T_1} \right) \log \frac{K_{C2}}{K_{C1}}, \tag{10}$$

$$\Delta S^\circ = \frac{\Delta H^\circ - \Delta G^\circ}{T}, \tag{11}$$

where C_A is the equilibrium concentration of the dye ions on adsorbent (mg·L^{-1}); C_S is the equilibrium concentration of the dye ions in the solution (mg·L^{-1}); R is the gas constant, T is temperature on the absolute scale and K_C, K_{C1}, and K_{C2} are the equilibrium constants at temperature T, T_1 and T_2, respectively.

The values of these parameters were calculated and are presented in Table 3. The values of ΔG° of dye/ZM adsorption systems are all negative, which indicates the spontaneous adsorption processes. Moreover, the increase in the absolute value of ΔG° with increasing temperature indicates that higher temperatures facilitated the adsorption. The positive value of ΔH° indicates that the adsorptions of both dyes onto ZM are endothermic. The positive value of ΔS° suggests that in the dye/ZM adsorption systems, although the adsorption process caused an entropy decrease for the adsorbed dye molecules, the entropy increase of dye molecules in dissolved state due to rising temperature was much greater, and consequently the ΔS° of the whole adsorption system increased.

Table 3: Thermodynamic parameters for adsorption of both dyes onto zeolite from fly ash-iron oxide magnetic nanocomposite.

Dye	T(K)	ΔG°(kJ·mol^{-1})	ΔH°(kJ·mol^{-1})	ΔS°(J·K^{-1}·mol^{-1})
	298	-0.71	74.0	250.5
RL16	303	-1.96	13.2	50.2
	313	-2.46		
	298	-0.44	1.83	7.60
IC	303	-0.47	22.7	76.4
	313	-1.24		

4 Conclusions

Zeolite from fly ash/iron oxide nanocomposite was investigated for the removal of reactive orange 16 (RO16) and indigo carmine (IC) from aqueous solutions. Adsorption processes for the two anionic dyes were found to follow the pseudo-second-order kinetics rate expression. Freundlich isotherm described the equilibrium data of IC on zeolite better than Langmuir isotherm, while Langmuir isotherm fitted better to the equilibrium data of RO16. Thermodynamic parameters were calculated and indicated that each of these adsorption processes was spontaneous and endothermic in nature. If magnetic zeolite/iron oxide nanocomposite is used as the adsorbent for dyes, magnetic separation will be applied and the clear solution could be easily decanted off or removed by pipette. Furthermore, supporting of magnetite nanoparticles on zeolitic material from coal fly ashes during the preparation process prevents the coaggregation of the iron oxide nanoparticles and is of help for their storage and pelletization.

References

[1] M. Yamaura, R. L.Camilo, and M. C. F. C. Felinto, J. Alloys Compd. 344 (2002) 152.
[2] Z. H. Ai, Y. Cheng, L. Z. Zhang, and J. R. Qiu, Environ. Sci. Technol. 42 (2008) 6955.
[3] S. Pal and E. C. Alocilja, Biosens. Bioelectron. 24 (2009) 1437.
[4] K. P. Singh, S. Gupta, A. K. Singh, and S. Sinha, J. Hazard Mater. 186 (2011) 1462.
[5] S.M. Yakout and M.M.S. Ali, J. At. Mol. Sci. 2 (2011) 117.
[6] A. Hanafi, J. At. Mol. Sci. 2 (2010) 292.
[7] Q. L. Zhang, Y. C. Lin, X. Chen, and N. Y. Gao, J. Hazard. Mater. 148 (2007) 671.
[8] P. Yuan, M. Fan, D. Yang, *et al.*, J. Hazard. Mater. 166 (2009) 821.
[9] G. S. Zhang, H. J. Liu, R. P. Liu, and J. H. Qu, J. Colloid Interface Sci. 335 (2009) 168.
[10] Y. Feng, J. L. Gonga, G. M. Zeng, *et al.*, Chem. Eng. J. 162 (2010) 487.
[11] L. C. A. Oliveira, R. V. R. A. Rios, J. D. Fabris, *et al.*, Carbon 40 (2002) 2177.
[12] L. C. A. Oliveira, R. V. R. A. Rios, J. D. Fabris, *et al.*, Appl. Clay Sci. 22 (2003) 169.
[13] L. C. A. Oliveira, D. I. Petkowicz, A. Smaniotto, and S. B. C. Pergher, Water Res. 38 (2004) 3699.
[14] D. A. Fungaro, M. Bruno, and L. C. Grosche, Desalin. Water Treat. 2 (2009) 231.
[15] D. A. Fungaro, L. C. Grosche, A. S. Pinheiro, *et al.*, Orbital Elec. J. Chem. 2 (2010) 235.
[16] D. A. Fungaro and J. E. A. Graciano, Adsorpt. Sci. Technol. 25 (2007) 729.
[17] D. A. Fungaro, M. Yamaura, and J. E. A. Graciano, Quim. Nova 33 (2010) 1275 (in Portuguese)
[18] T. Henmi, Clay Sci. 6 (1987) 277.
[19] Y. S. Ho, Carbon 42 (2004) 2115.
[20] Y. S. Ho and G. McKay, Can. J. Chem. Eng. 76 (1998) 822.
[21] Y. S. Ho, D. A. J. Wase, and C. F. Forster, Environ. Technol. 17 (1996) 71.
[22] W. J. Weber and J. C. Morris, J. Sanit. Engin. Div. ASCE 89 (1963) 31.
[23] Y. S. Ho, Water Res. 37 (2003) 2323.
[24] S. J. Allen, G. McKay, and K. Y. H. Khader, Environ. Pollut. 56 (1989) 39.

[25] N. Dizge, C. Aydiner, E. Demirbas, *et al.*, J. Hazard. Mater. 150 (2008) 737.
[26] W. H. Cheung, Y. S. Szeto, and G. McKay, Bioresour. Technol. 98 (2007) 2897.
[27] K. G. Bhattacharyya and A. Sharma, Dyes Pigm. 65 (2005)51.
[28] W. A. Helby, Chem. Eng. 59 (1952) 153.
[29] B. Acemioglu, J. Colloid Int. Sci. 274 (2004) 371.
[30] G. Atun, G. Hisarlý, A. E. Kurtoglu, and N. Ayar, J. Hazard. Mater. 187 (2011) 562.
[31] A. Sharma and K. G. Bhattacharyya, Indian J. Chem. Technol. 12 (2005) p. 285.
[32] E. Gutierrez-Segura, M. Solache-Rios, and A. Colin-Cruz, J. Hazard. Mater. 170 (2009) 1227.
[33] M. B. Kasiri, H. Aleboyeh, and A. Aleboyeh, Appl. Catal. 84 (2008) 9.
[34] C. Namasivayam and R. T. Yamuna, Environ Pollut. 89 (1995) 1.
[35] C. Namasivayam, N. Muniasamy, K. Gayathri, *et al.*, Biores Technol. 57 (1996) 37.
[36] C. Namasivayam, D. Prabha, and M. Kumutha, Bioresour. Technol. 64 (1998) 77.
[37] A. Shukla, Y. H. Zhang, P. Dubey, *et al.*, J. Hazard. Mater. 95 (2002) 137.
[38] B. Royer, N. F. Cardoso, E.C. Lima, *et al.*, J. Colloid Interface Sci. 336 (2009) 398.